Corrosion Science 134 (2018) 131–139

Contents lists available at ScienceDirect

Corrosion Science

journal homepage: www.elsevier.com/locate/corsci

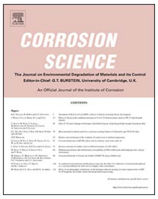

Short Communication

Corrosion behavior of an equiatomic CoCrFeMnNi high-entropy alloy compared with 304 stainless steel in sulfuric acid solution

Hong Luo*, Zhiming Li*, Andrea M. Mingers, Dierk Raabe

Max-Planck Institut für Eisenforschung, Max-Planck Str. 1, D-40237 Düsseldorf, Germany

ARTICLE INFO

Keywords:
A. Alloy
B. XPS
C. Corrosion
C. Acid corrosion

ABSTRACT

The corrosion resistance and passive film properties of an equiatomic CoCrFeMnNi high-entropy alloy (HEA) compared with 304L stainless steel in 0.1 M H_2SO_4 solution were investigated. The in-situ element-resolved corrosion analysis shows that selective dissolution of elements in the HEA is not evident compared to a 304 L stainless steel during passivation. The passive film formed on the HEA is enriched in Fe and Mn but depleted in Cr. The low content of Cr and the extensive formation of metal hydroxide in the passive film are responsible for the lower anti-corrosion performance of the HEA.

1. Introduction

High-entropy alloys (HEAs) were originally designed as alloys composed of multiple principal elements in equimolar or near-equimolar ratios where the high mixing entropy serves in stabilizing them in disordered massive solid solution state [1,2]. Over the past decade, this concept has attracted considerable attention as it provides enormous compositional opportunities for designing novel materials with beneficial mechanical properties [3–5]. Accordingly, various HEAs have been developed during the past years, e.g., face-centered cubic (FCC) CoCrFeMnNi [6] and body-centered cubic (BCC) VNbMoTaW [7] alloy systems. Among these, the FCC structured equiatomic CoCrFeMnNi HEA which was first reported by Cantor et al. [2], has particularly excellent mechanical properties at cryogenic and room temperature [4].

Recently, the corrosion behavior of some types of HEAs in aqueous solution has been reported. Shih et al. [8] revealed that the corrosion resistance of $Al_xCrFe_{1.5}MnNi_{0.5}$ (x = 0, 0.3, 0.5 at.%) HEAs in H_2SO_4 and NaCl solutions enhances as the concentration of aluminium decreases from 0 to 0.5 at.%. The pitting corrosion behavior of a $Co_{1.5}CrFeNi_{1.5}Ti_{0.5}Mo_{0.1}$ HEA in chloride-containing sulphate solutions studied by Yeh et al. shows that the values of the pitting potential change in a linear manner with the logarithm of the chloride concentration at 70 °C and 80 °C [9]. Moreover, the influence of the Al content on stable/metastable pitting of an $Al_xCoCrFeNi$ (x = 0.3, 0.5, 0.7 at.%) HEA in a 3.5 wt.% NaCl solution was investigated by Liwa [10]. Also, Grewal, et al. [11] demonstrated the cavitation erosion-corrosion behavior of the $Al_{0.1}CoCrFeNi$ HEA in 3.5 wt.% NaCl. Very recently, Rodriguez et al. [12] investigated the corrosion behavior of the group of CoCrFeMnNi HEAs in acidic sodium chloride solution with CO_2. They showed that the Cr content plays an important role on the corrosion rate of the HEAs. In addition, the corrosion properties of the CoCrFeMnNi HEA coating in 3.5 wt.% NaCl solution has been evaluated [13] and it was shown that the element segregation exhibits harmful effects on the corrosion resistance of the HEA coating.

It is well known that the surface of binary Fe-Cr alloys can be rendered passive when the Cr content is above 12 at.% [14]. The excellent corrosion resistance of austenite stainless steels with a Cr content above 12 at.% is also due to the formation of a protective thin passive film on its surface when exposed to the corrosive environment [15]. The corrosion and electrochemical behavior of stainless steel in various environments have been well characterized [15–18]. Interestingly, the equiatomic CoCrFeMnNi HEA contains similar corrosion-resistant elements, i.e., Cr and Ni as the standard AISI 304 austenite stainless steel (72Fe-19Cr-9Ni). Also, they both have a single-phase FCC structure with similar lattice parameter (~0.36 nm [19]). Although very recently Rodriguez et al. [12] investigated the corrosion properties of the CoCrFeMnNi HEA family in acidic sodium chloride solution, detailed information such as the fundamental mechanisms associated with the composition and structure of the passive film are still unknown. Yet it is of interest to fundamentally understand the corrosion behavior of the equiatomic CoCrFeMnNi HEA in comparison with the well-established 304L SS considering their similar corrosion-resistant elements (Cr and Ni) and single FCC lattice structure.

Motivated by the above considerations, in this work we investigated the corrosion behavior of the equiatomic CoCrFeMnNi HEA compared with the 304 L stainless steel in 0.1 M H_2SO_4 solution by combining a micro-electrochemical scanning flow cell (SFC) and an inductively

---

* Corresponding authors.
E-mail addresses: h.luo@mpie.de (H. Luo), zhiming.li@mpie.de (Z. Li).

https://doi.org/10.1016/j.corsci.2018.02.031
Received 13 June 2017; Received in revised form 9 February 2018; Accepted 16 February 2018

Table 1
Compositions of HEA and 304L SS according to wet-chemical analysis (wt.%).

Elements	C	Cr	Ni	P	S	Co	Mn	Fe
HEA	–	18.6	20.9	–	–	21.1	19.5	19.9
304 L SS	0.006	18.15	8.04	0.015	0.005	–	0.35	73.43

coupled plasma mass spectroscopy (ICP-MS) element analysis. The passivation behavior and composition of the passive film of the equiatomic CoCrFeMnNi HEA were investigated by electrochemical impedance spectroscopy (EIS) and X-ray photoelectron spectroscopy (XPS), respectively. Our main aim is to identify the corrosion mechanism of the equiatomic CoCrFeMnNi HEA.

2. Experimental procedures

2.1. Sample preparation

The equiatomic CoCrFeMnNi HEA was cast in a vacuum induction furnace using high purity metals. The cast ingot was hot-rolled at 900 °C to a thickness reduction of 50%, and then homogenized at 1200 °C for 2 h in Ar atmosphere followed by water-quenching. To refine the grain size, HEA samples were cold-rolled to a thickness reduction of 60%, and subsequently annealed at a furnace temperature of 900 °C for 5 min in Ar atmosphere followed by water-quenching. A commercial 304L SS (stainless steel) sheet with a thickness of 2 mm was used as reference material. The chemical compositions (wt.%) of the two types of materials investigated are listed in Table 1. Samples with dimensions 10 mm × 10 mm × 2 mm were machined from the alloy sheets. Then, they were ground sequentially from 400 to 2500 grit SiC paper, polished with 0.1 μm diamond powder. After that, they were cleaned with deionizer water, alcohol, and then dried in cool air. The electrodes used for the electrochemical tests were connected by a wire welded to the back side of the samples, and sealed with a curing epoxy resin, leaving only one face with a size of 1 cm^2 exposed to the solution. 0.1 M H_2SO_4 solution was used as electrolyte during the testing.

2.2. Microstructural analysis

The starting microstructures of the materials were characterized by back-scatter electron imaging (BSEI) and electron backscatter diffraction (EBSD) using a Zeiss-Merlin and a Zeiss-Crossbeam XB 1540 FIB scanning electron microscope (SEM), respectively. X-ray diffraction (XRD) analysis were conducted using an X-Ray equipment ISO-DEBYEFLEX 3003 equipped with Co Kα ($\lambda = 1.788965$ Å) radiation operated at 40 kV and 30 mA.

2.3. Micro-electrochemical corrosion and online in-situ element-resolved analysis

Micro-electrochemical corrosion and online element-resolved measurements were performed in 0.1 M H_2SO_4 (Merck, 96% suprapur) using a scanning flow cell (SFC) with a potentiostat Gamry Reference 600 at ambient pressure and temperature (25 °C). The tip of the microcell was encircled by a silicone O-ring that prevents electrolyte leakage when the cell is pressed onto the sample connected as working electrode. The area that was wetted by the cell was about 1.08 mm^2. The counter electrode (Pt-wire, 0.5 mm, 99.997%, Alfa Aesar) was placed in the inlet channel and the reference electrode (Ag/AgCl, 3 M KCl, reference potential +207 mV vs. standard hydrogen electrode (SHE)) in the outlet channel of the cell. The electrolyte outlet of the SFC was connected to the inductively coupled plasma-mass spectrometer (ICP-MS, NexION 300X, Perkin Elmer) for online in-situ element-resolved analysis. The electrolyte was pumped through the cell at a flow rate of 230 $\mu L\ min^{-1}$. The ICP-MS was calibrated prior to the measurements. The detected intensities of the elements (^{52}Cr, ^{55}Mn, ^{56}Fe, ^{59}Co, ^{60}Ni) were converted to the concentration of dissolved ions. Detailed setup and measurement processes were described in the literature [20]. During the ICP-MS measurement, the concentrations of dissolved ions were detected for three different stages, i.e., open-circuit potential (OCP), holding time and polarization. Between the OCP and polarization stages, a holding time of approximately 5 min was required to ensure a stable testing system. In addition, the cyclic potentiodynamic polarization tests were performed at a scan rate of 0.1 $mV\ s^{-1}$ with a specimen surface area of 1.0 cm^2. A saturated KCl, Ag/AgCl reference electrode was connected to the cell through a Luggin capillary. All potentials in the present study refer to SHE. The electrochemical impedance spectroscopy (EIS) measurements were conducted in a Solartron system-potentiostat (model 1287A)/frequency response analyzer (model 1260A) workstation with a conventional three-electrode cell. Before the EIS tests, the OCP was measured for 3600 s. The EIS was started with the applied AC amplitude of 10 mV, and the frequency was swept from 100 kHz down to 10 mHz. The impedance data was interpreted by using the Zsimpwin software and equivalent electron circuits. Each experiment was repeated at least three times under the same condition to confirm reproducibility. All EIS measurements were conducted at room temperature (25 °C).

2.4. Compositional analysis of the passive films

To investigate the passive films on the equiatomic HEA and 304L SS, the bulk samples were charged under potentiostatic conditions for 2 h at a potential of +400 mV_{SHE} to produce the stable passive films. The potential was chosen with reference to the characteristic features of the potentiodynamic polarization curve. Then, the specimens were rinsed with distilled water, dried and transferred to the X-ray photoelectron spectroscopy (XPS) analyzer chamber immediately. The compositions of the passive films formed by exposing the specimens to the 0.1 M H_2SO_4 solution were measured by using a Physical Electronics Quantum 2000 ESCA microprobe system in conjunction with monochromatic Al K_α X-ray radiation. The XPS data were analyzed using the commercial software CasaXPS (version 2.3.15), and the peaks were fitted by the mixed Gaussian-Lorentzian functions after Shirley background subtraction. The binding energy (BE) scale was calibrated on a C1 s peak at 285 eV, and all the other peaks obtained by the XPS analysis were calibrated by the standard C1 s peak. XPS analysis for each sample condition was repeated at least three times to confirm reproducibility.

2.5. Immersion tests and surface observation

Immersion tests were carried out in 0.1 M H_2SO_4 solution at room temperature for 30 days. Then, the surface morphology of the tested samples was investigated by using Zeiss-Merlin instrument equipped with energy-dispersive spectrometry (EDS).

3. Results and discussion

3.1. Starting microstructure

Fig. 1 show the inverse pole figure (IPF) maps and back-scattered electron (BSE) morphology of the equiatomic CoCrFeMnNi HEA and 304 L SS, respectively. Both types of materials exhibit recrystallized microstructure with high amounts of annealing twins. The XRD patterns inserted in Fig. 1b_2 confirm the FCC structure with similar lattice parameters in both materials. The average grain sizes of the CoCrFeMnNi HEA and the 304 L SS are ~8 μm and 30 μm, respectively. According to the previous work, grain size, when in the micrometer-range, has no substantial effect on the corrosion of stainless steel [21,22] in sulfuric acid solution. An evident influence occurs only when the average grain size value falls into the nanoscale regime [23,24]